Introduction to Optical Tweezers: Background, System Designs, and Applications

Malinowska, A.M.; van Mameren, J.; Peterman, E.J.G.; Wuite, G.J.L.; Heller, I.

DOI
10.1007/978-1-0716-3377-9_1

Publication date
2024

Document Version
Final published version

Published in
Single Molecule Analysis

Chapter 1

Introduction to Optical Tweezers: Background, System Designs, and Applications

Agata M. Malinowska, Joost van Mameren, Erwin J. G. Peterman, Gijs J. L. Wuite, and Iddo Heller

Abstract

Optical tweezers are a means to manipulate objects with light. With the technique, microscopically small objects can be held and steered, allowing for accurate measurement of the forces applied to these objects. Optical tweezers can typically obtain a nanometer spatial resolution, a picoNewton force resolution, and a millisecond time resolution, which makes the technique well suited for the study of biological processes from the single-cell down to the single-molecule level. In this chapter, we aim to provide an introduction to the use of optical tweezers for single-molecule analyses. We start from the basic principles and methodology involved in optical trapping, force calibration, and force measurements. Next, we describe the components of an optical tweezers setup and their experimental relevance. Finally, we will provide an overview of the broad applications in context of biological research, with the emphasis on the measurement modes, experimental assays, and possible combinations with fluorescence microscopy techniques.

Key words Optical tweezers, Optical trap, Single molecule, Fleezers, Trap stiffness calibration, Force spectroscopy, Instrument design, Molecular motors, DNA-protein interactions

1 Introduction

1.1 History of Optical Tweezers

At the heart of optical tweezers techniques is the interaction between light and matter. The minute forces that are generated in this interaction can be used to displace and trap microscopic objects. In 1970, Arthur Ashkin laid the foundations for present-day optical tweezers techniques when he observed that micrometer-sized latex beads were attracted toward the center of an argon laser beam [1]. In addition to this inward movement of the beads, Ashkin also noticed that the laser light scattered and propelled the beads forward. By combining two counter propagating beams, he managed to avoid forward propulsion, and thus, he created the first stable optical trap for beads suspended in water. In 1986, Ashkin together with Chu demonstrated optical trapping with a single, tightly focused laser

Iddo Heller et al. (eds.), *Single Molecule Analysis: Methods and Protocols*, Methods in Molecular Biology, vol. 2694,
https://doi.org/10.1007/978-1-0716-3377-9_1,

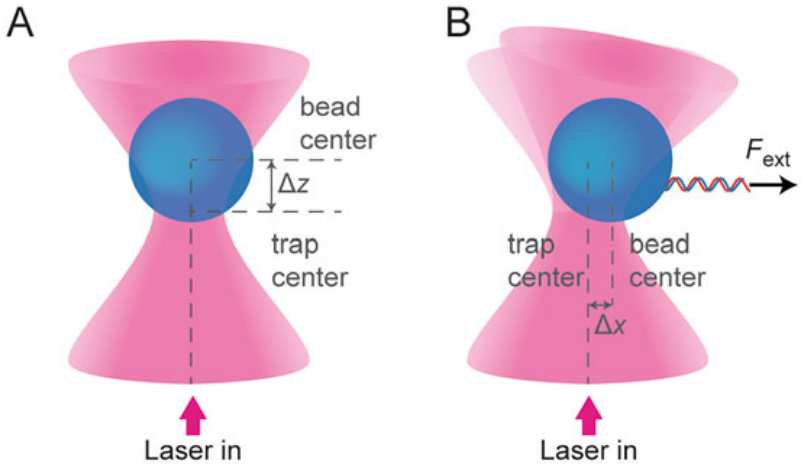

Fig. 1 Schematic of optical trapping. *Left*: a tightly focused laser beam (cone) attracts refractive objects (blue sphere) such as glass beads, nanoparticles, or even whole cells to its focus, though the momentum of photons pushes the object slightly forward. *Right*: external forces pushing or pulling on the particle slightly displace it from the center of the focus, leading to a slight deflection of the forward scattered laser light. This deflection forms the basis for quantitatively detecting the forces and displacements experienced by the trapped object (Adapted with permission from Heller et al. [8]. Copyright 2014 American Chemical Society)

beam. At present, single-beam optical trapping is the most commonly used form of optical tweezers, which allows for stable trapping of particles with diameters between 25 nm and 10 μm, in three dimensions (Fig. 1) [2]. Later on, Chu and others used techniques inspired by optical tweezers to trap and cool atoms, which brought him the 1997 Nobel Prize in physics [3, 4]. At age 96, Ashkin became the oldest Nobel prize winner when he was recognized for his invention of optical tweezers and their application to biological systems by receiving the 2018 Nobel Prize in physics.

1.2 Optical Tweezers in Biology

Currently, optical tweezers have found widespread applications in biology [5–8]. One of the important reasons for the success of optical tweezers is that it provides scientists with "microscopic hands" to manipulate biological objects and measure and exert forces, yet with the same low level of invasiveness as light microscopy techniques. Furthermore, the length scales, time scales, and force scales accessible to optical tweezers are biologically relevant from the single-cell level down to the single-molecule level. In 1987, Ashkin presented the first applications of optical tweezers in biology: through the careful choice of laser power and wavelength, photodamage could be minimized, which allowed trapping and manipulation of viruses, bacteria, and single living cells [9, 10]. Since these first demonstrations of optical tweezers in biology, optical tweezers approaches have been extended down to the single-molecule level [11–22]. In such single-molecule studies, the biomolecules of interest are not trapped directly, but they are

tethered to optically trapped microbeads that act as handles and force transducers. Several assays and pulling geometries have been employed over the years, each representing different technological or methodological characteristics (Fig. 2).

A large fraction of single-molecule optical tweezers analyses involves studying the activity of individual motor proteins [11, 15, 22]. With optical tweezers, the motion and forces generated by these motor proteins have been studied and controlled to reveal their dynamics and energetics (Fig. 2a). Another important area of research is the study of biopolymers such as DNA [7, 14, 18, 23, 24]. In these experiments, one end of the DNA molecule is attached to an optically trapped bead, while the other end is attached to a substrate (Fig. 2b), to a bead that is held by a micropipette (Fig. 2c), or to a bead that is held in a second optical trap (Fig. 2d). In such stretching assays, the extension of the DNA molecule and its tension can be controlled and/or measured concurrently, which allows for studying its mechanical properties. This layout has been used to also study proteins and DNA-protein interactions [13, 17, 21, 25–27]. A wide range of proteins that interact with DNA can alter the mechanical properties of DNA and thus the (force-dependent) length of the DNA molecules and/or force response of the biopolymer [13, 28, 29]. In optical tweezers, these length changes can be observed by measuring the displacements of the microbeads. Examples include the study of DNA-binding proteins and the activity of DNA and RNA polymerases [8, 13, 17].

An extension of the dual-trap optical tweezers is a quadruple-trap setup, which allows manipulating two DNA molecules independently (Fig. 2e). This approach is convenient for experimentation on proteins that interact with multiple strands of DNA such as cross-linking ligands [25, 30] or complex assays with two intertwined DNA strands [31, 32].

Over the last decade, the impact of optical tweezers in biology has further expanded due to their integration with other experimental techniques. This includes their combination with multichannel microfluidics, which not only enhances experimental throughput but also provides in situ control of more complex multistep biological processes [33, 34]. Most notably, the combination of optical tweezers with the rich arsenal of fluorescence techniques has enabled optical tweezers analyses to venture far beyond strictly mechanical measurements, as we describe in Subheading 4.3 [8, 33, 35].

With the advent of commercial optical tweezers systems in recent years, this powerful single-molecule technique is approaching maturation and is becoming more and more common in biomolecular research. Analogous to commercialization of fluorescence microscopy and AFM techniques, it is to be expected that commercial optical tweezers will further accelerate our progressive understanding of biological processes at the single-molecule level.

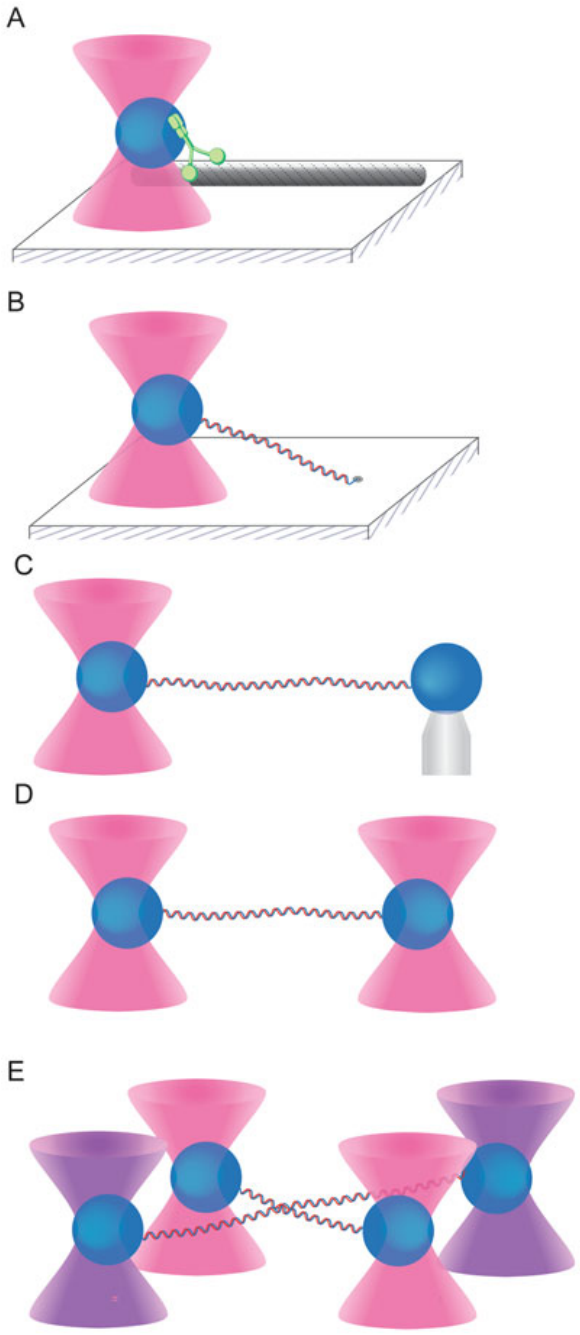

Fig. 2 Prototypical single-molecule optical tweezers assays and pulling geometries. (**a**) A single kinesin motor protein bound with its two heads to an optically trapped bead moves along a surface-immobilized microtubule track. Its 8-nm steps, the forces exerted, and the mechanics of the stepping have been elucidated in such assays. (**b**) DNA anchored between an optically trapped bead and the surface. (**c**) DNA tethered between an optically trapped bead and a bead that is held in a micropipette; (**d**) DNA suspended between two optically trapped beads—this so-called dumbbell approach allows maneuverability through a flow cell to, for example, rapidly move between parallel laminar flow lanes. (**e**) Quadruple-trap optical tweezers assay in which two DNA strands are manipulated concurrently (Adapted with permission from Heller et al. [8]. Copyright 2014 American Chemical Society)

2 Principles of Optical Tweezers Techniques

The basic physical principle underlying optical tweezers is the radiation pressure, exerted by light when colliding with matter. For macroscopic objects, the radiation pressure exerted by common light sources is orders of magnitude too small to have any measurable effect: we do not feel the light power of the sun pushing us away. However, for objects of microscopic dimensions (<100 μm), the radiation pressure of high intensity light sources is sufficient to facilitate optical trapping.

2.1 Forces in an Optical Trap

When photons enter an object that has a different refractive index than its surrounding medium, part of the momentum of the photons can be transferred to this object. This transfer of momentum is the physical principle that underlies optical trapping (see Fig. 1b). The forces exerted by photons on an optically trapped object can be divided into two components: the scattering force that pushes the object away from the light source and the gradient force that pulls the object toward the region of highest light intensity. The correct physical description of optical trapping depends on the size d of the trapped object in comparison to the wavelength λ of the trapping light. In the regime where $d >> \lambda$, one speaks of the "ray-optics" regime, while the regime where $d << \lambda$ is called the Rayleigh regime. Micrometer-sized beads trapped in biological experiments can be placed between these two regimes; thus, neither description is quantitatively accurate. To provide a qualitative understanding of optical trapping, we will here describe the forces in the more intuitively interpretable ray-optics regime. In the ray-optics regime, the trapping force can be understood in terms of refraction of light rays between media with different indices of refraction [36]. Figure 3 qualitatively depicts the origin of the trapping forces in this regime. The lateral gradient restoring force (Fig. 3a) can be understood as follows. If two rays have different intensity ("bright" and "dim"), the momentum changes of these rays will differ in magnitude, and conservation of momentum of the photons will result in a net reaction force on the refracting medium (or object) in the direction of highest intensity. The x–projection of this force, Δp, tends to counteract a displacement from the laser beam axis, pulling the particle toward the center of the beam. The axial gradient force F_{gr} is similarly caused by momentum transfer upon refraction, resulting in a restoring force toward the focus, as in Fig. 3b. On the other hand, the scattering force F_{sc} will cause the object to be propelled out of the focus, along the positive z–direction. The object is stably trapped only if the scattering force along the positive z–direction is compensated by the gradient force along the negative z–direction. To achieve this, a significant fraction of the incident light should come in at large angles, calling for a tightly focused trapping light source, typically obtained by using a

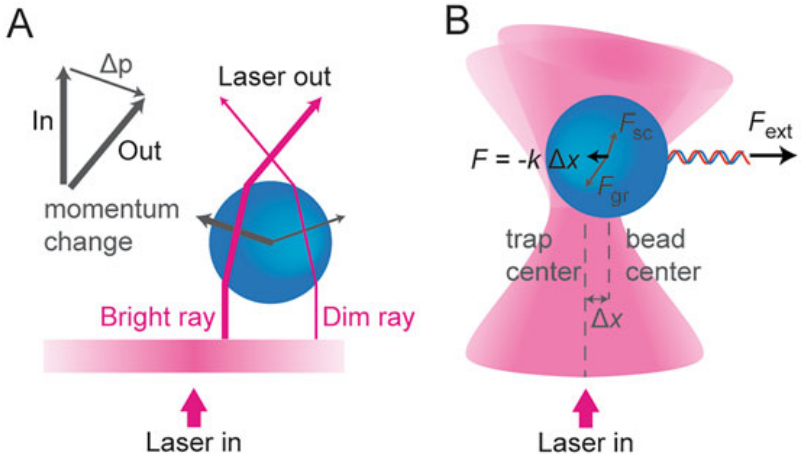

Fig. 3 Forces on an optically trapped particle in the ray-optics regime. (**a**) Lateral gradient force of a Gaussian laser beam profile. (**b**) Axial gradient force toward the focus of the trapping light. The thick black arrow indicates the net restoring force. Note that the scattering component due to reflection by the particle is not indicated

microscope objective with high numerical aperture. When an external force F_{ext} is acting on a bead (i.e., by pulling on the DNA), the bead will be displaced from the equilibrium position in the center of the trap. For moderate displacements Δx, the trap behaves like a linear spring, and the net restoring force F obeys Hooke's law $F = -\kappa\Delta x$. Here, κ denotes the spring constant in units of [N/m] and signifies the stiffness of the optical trap. Knowledge of the trap stiffness allows accurate quantification of the external forces acting on a trapped particle from a measurement of the particle's displacement. The trap stiffness, however, depends on the intensity profile and wavelength of the laser, the shape and size of the trapped particle, the indices of refraction, and many other parameters, making it difficult to calculate from first principles. Therefore, the trap stiffness is commonly determined by performing calibration experiments. Using a 1064 nm laser of 1 W, the typical trap stiffness that can be obtained in a single-beam optical trap is in the order of 100 pN/μm.

2.2 Principles of Trap Calibration

To allow quantitative measurement of the forces on optically trapped particles, several calibration methods to measure the trap stiffness have been developed.

Drag Force Calibration The simplest way to calibrate an optical trap is to apply an external force of known magnitude and measure the displacement of the trapped particle. The external force is typically generated by inducing a fluid flow. The drag force of the fluid (viscosity η, flow velocity v) acting on a spherical bead of diameter d is given by Stokes' law: $F = \gamma v$, where γ is the drag coefficient $\gamma = 3\pi\eta d$. The fluid drag displaces the bead from the

center of the trap until the drag force is equal to the opposing restoring force from the optical trap, which yields $\kappa = \frac{\gamma v}{x}$. The trap stiffness can thus be obtained by measuring the displacement, x, of a bead of known size due to the fluid flow of a liquid with known viscosity and velocity.

Brownian Motion Calibration Another more accurate calibration procedure is based on the Brownian motion of a bead in an optical trap. The stiffness of an optical trap can be estimated by recording the power spectrum of the displacement fluctuations of a trapped bead of known size, as shown in Fig. 4. The power spectrum $S_x(f)$ describes how the power of these displacement fluctuations is distributed with respect to frequency f and has a Lorentzian shape [37]:

$$S_x(f) = \frac{k_B T}{\gamma \pi^2 \left(f_c^{\,2} + f^2\right)},$$

where $k_B T$ is the available thermal energy. The power spectrum exhibits a characteristic corner frequency $f_c \equiv \kappa/2\pi\gamma$, which is proportional to the trap stiffness. Figure 4 shows that at low frequencies $f << f_c$, the power spectrum is roughly constant,

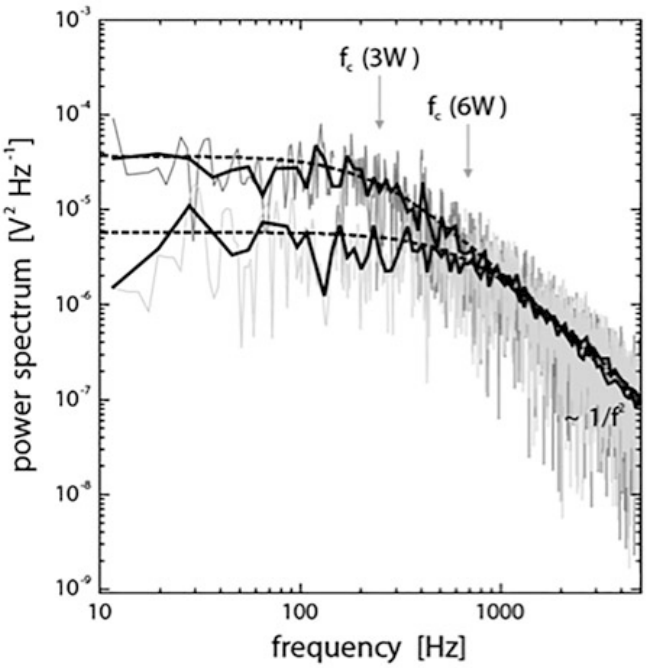

Fig. 4 Power spectra representative of the positional fluctuations of a particle trapped at different laser powers. A 1 μm diameter polystyrene bead is held in an optical trap, while the displacement signal in volts is sampled at 195 kHz. The graph shows power spectra of the displacement signal at 3 W (dark gray) and at 6 W (light gray) laser power. Both the downward shift of the low-frequency plateau S_0 and the upward shift of the corner frequency f_c (see arrows at 250 Hz and 650 Hz, obtained from Lorentzian fits) for the stiffer 6 W trap can clearly be observed

$S_x(f) = S_{x,0} = 4\gamma k_B T/\kappa^2$. At high frequencies $f >> f_c$, however, the power spectrum falls off like $1/f^2$, which is a characteristic of free diffusion. The inverse of the corner frequency represents the time response of the optical trap, which is typically in the order of 1 ms to 0.1 ms. For shorter time scales, the particle does not "feel" the confinement of the trap, which means that behavior of biological systems at time scales more rapid than this response time cannot be detected by the optical tweezers (*see* **Note 1**). The two power spectra of Fig. 4, acquired at two different trap stiffness values, illustrate that when a higher trap stiffness is used (i.e. by increasing the laser power), the bead fluctuations at low frequencies are reduced, and the time response of the optical trap increases. On the other hand, a higher trap stiffness implies smaller bead displacement at a given force, which implies that there is not necessarily an improvement in signal-to-noise ratio at elevated trap stiffness [38]. Typical parameters to consider for improving the signal-to-noise ratio in force or distance measurements include using a stiff tether (e.g., shorter DNA construct or elevated tension) and/or time averaging the measurement signal. Using small beads can be of additional benefit: the faster fluctuations of small beads are more effectively filtered out by time averaging than those of large beads. Large beads, on the other hand, have the advantage that the trapping laser is focused inside the bead, where it is far away from biomolecules of interest such that potential photo-damage can be minimized (*see* Subheading 4.3 on combined optical trapping and fluorescence microscopy).

3 Optical Tweezers Systems

An optical tweezers setup consists of several optical elements that require optimal alignment to guarantee the best performance of the instrument. Additional components facilitate experimental workflows and create an optimal low-noise and low-drift working environment. Below, we divide and discuss the components in *five groups: the trap, the environment of the trap, trap steering, position and force detection, and the environment of the setup*. For illustration, Fig. 5 shows the schematic layout of an optical tweezers setup that combines two steerable optical traps with fluorescence microscopy.

3.1 The Optical Trap

At the heart of every single-beam optical tweezers instrument is the *microscope objective*, which creates the tight focus that is required to form a stable optical trap. Tight focusing implies that a significant fraction of the incident light comes in at large angles, such that the scattering force is overcome by the gradient force. The maximum incidence angle of the light Θ_{max} is determined by the numerical aperture (NA) of the objective used to focus the laser beam. This is

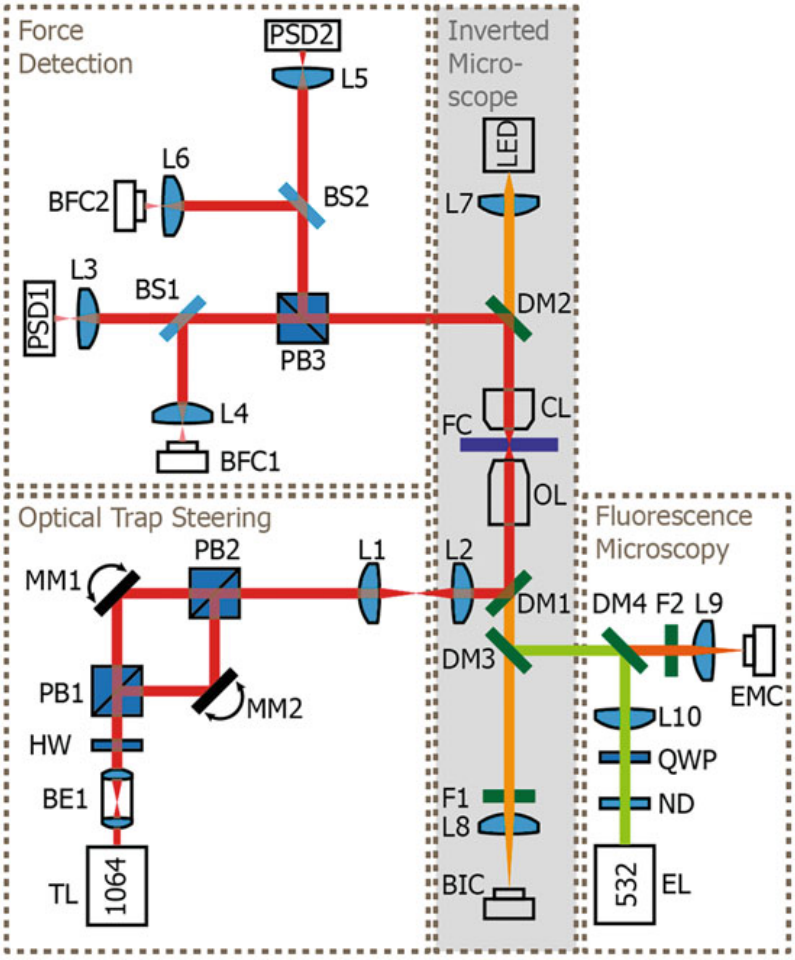

Fig. 5 Optics layout of a typical optical tweezers–fluorescence instrument. The various parts of the system as described in the text are bounded by dashed boxes. The optics are divided into four functional units: in the Optical Trap Steering Unit, two continuously illuminated optical traps are created from a high power 1064 nm trapping laser (TL) using polarizing beamsplitter cubes (PB1-2) and a half-wave plate (HW). Each trap is steered using a dedicated motorized mirror (MM1-2) located in planes conjugate to the back-focal plane of the objective lens (OL). Beam expander BE1 allows changing the collimation of the traps and change their axial position. In the Force Detection Unit, two position sensitive detectors (PSD1–2) monitor the force and displacement of two orthogonally polarized traps. The Inverted Microscope Unit is based on a commercial microscope body and uses a point-source LED to illuminate the sample plane that is imaged on a bead imaging camera (BIC). The Fluorescence Microscopy Unit consists of a simple wide-field layout where an excitation laser (EL) illuminates the sample while the fluorescence signal is imaged onto an EMCCD (EMC). Diagnostic tools added include the two cameras that image the condenser's back-focal plane (BFC1,2). BS beam splitter, CL condenser lens, FC flow cell, L lens, ND neutral density filter, QWP quarter-wave plate

a measure for the solid angle over which the objective lens can gather light and is defined as NA = n sin Θ_{max}, where n is the refractive index of the immersion medium (in this case the medium between the objective lens and the sample) and Θ_{max} is one-half the angular aperture. The value of n varies between 1.0 for air and ~1.5 for most immersion oils. For typical oil-immersion objectives, an NA of 1.4 corresponds to a total acceptance angle of the objective of about 130 degree. To obtain a stable three-dimensional optical trap, the laser beam entering the objective has to be wide enough to fill or overfill the back aperture of the objective. This way, one provides sufficient convergent, high-angle rays that contribute to counteracting the scattering force.

The maximum force that can be exerted by an optimized focal spot of an optical trap can be increased by either increasing the laser power or by optimizing the refraction of the laser by the trapped particle. The laser power can only be increased up to a certain limit, above which more laser light would lead to heating or photodamage of the examined biological system, or even damage to the optics in the instrument [39]. The difference in refractive index of the trapped object n_2 compared to that of the surrounding medium n_1 determines how strongly the incident rays are refracted and, consequently, how strong the trapping force is. The required balance between gradient and scattering forces yields an optimal refractive index of $n_2 = 1.69$ [5]. For aqueous buffers, silica (glass) particles ($n_2 = 1.37–1.47$) or polystyrene particles ($n_2 = 1.57$) are most often used. The higher refractive index of polystyrene particles thus permits higher trapping forces. Recently, nanometer-sized germanium particles with a refractive index as high as 4.4 have been optically trapped. Efficient trapping of such small particles without excessive heating has set a new benchmark for concurrent spatial resolution and temporal response (i.e., spatiotemporal resolution) of optical tweezers [40].

When using an oil-immersion objective, the refractive index of the immersion oil matches both that of the objective lens and that of the glass of the sample, and the maximum NA can be achieved. However, due to the refractive index mismatch between the sample glass and the aqueous buffer, spherical aberrations deteriorate the quality of the laser focus when the distance of the focus to the sample surface increases (optical trapping in water with oil immersion objectives is typically performed within several (tens of) micrometers of the glass surface) [41]. To allow equally stable trapping at any distance to the surface, water-immersion objectives are often used. Despite the fact that the NA is somewhat lower (typically NA = 1.2 for water immersion objectives), the ability to move away from the sample surface without lowering the trap quality can be a good reason to use water-immersion objectives [42].

Most commonly used trapping lasers are single-mode continuous wave lasers with a Gaussian beam profile. The laser power typically ranges from a few hundred milliwatts up to several watts. Important in the context of stable trapping are low intensity fluctuations and high pointing stability (little angular and transverse wandering of the beam). For biological experiments, also the laser wavelength is of particular interest, as the light intensity at the focus of the trap is very high, which can lead to heating and damage of the often sensitive biological material. Near-infrared lasers (800–1200 nm, most often 1064 nm) are typically used, because of the low absorption of biological material and of water in this spectral range [5]. In addition, these wavelengths do not typically interfere with concurrent fluorescence microscopy.

Although in current biological applications optical traps are most commonly formed by tightly focusing a single laser beam [2], the first stable optical trap was accomplished in 1970 by using two counter-propagating focused laser beams [1]. The counter propagating layout does not require tight focusing, such that low NA (<1) objectives, or no objective at all may be used. Advantageously, this allows for a larger working distance and lower local light intensity at the trap, making it useful to handle living cells. The "optical stretcher," designed to probe the deformability of individual cells, is a key example of this approach [43].

3.2 Environment of the Trap

Microfluidics To ascertain well-controlled experimental conditions in single-molecule experiments, it is often useful —if not required— to implement a way to bring the biochemical "ingredients" together under the microscope. Use of microfluidics can facilitate the process by enabling fine control over the flow of minute volumes of the used solutions. The laminar flow within the flow cell ensures that different buffer flows can be in contact with each other with negligible mixing in relevant sections of the flow cell. In addition, microfluidic control allows for drag force calibration of the trap, as well as flow stretching of biopolymers such as DNA for easy tethering between beads [35]. An alternative way to induce viscous drag is by moving the fluid reservoir with respect to the trap using a motorized microscope stage. Particularly useful is the combination of either a motorized or a piezoelectric stage with a multichannel laminar flow cell. Moving the stage allows for swift change of the position of the trapped beads in the microfluidic chip, hence the buffer conditions can be rapidly and completely exchanged while using the same single-molecule construct. This facilitates in situ control of more complex multistep biological processes, and it enhances experimental throughput. Brewer et al. extensively reviewed the use of microfluidics devices in single-molecule experiments [34]. It is important to note here the additional benefit of the dual-trap setup, where the tethered

biopolymer is fully suspended in the solution and protected from unwanted surface interactions. This layout suppresses noise associated with fluctuations or drift in the relative positions of the optical trap and a fixed substrate, which provides additional flexibility in applications of the technique.

Temperature Stability In biological experiments, temperature often plays an important role. Similar to conventional microscopy instruments, optical tweezers can be easily combined with temperature-controlled fluidics, stages, and objectives. The high-NA objective lenses that are required to obtain a tight focus have relatively short focal lengths and are thus in close contact with the trapping region through the immersion medium, acting as an effective heat sink. As a result of this strong thermal coupling, the temperature of the trapping region is typically governed by the temperature of the objective (and condenser) lenses. It can thus be important to be aware of or control the objective (and condenser) temperature. Moreover, apart from the relevance of the temperature for the biological system, temperature control of the objective can be beneficial for the performance of the optical tweezers as well. The high laser intensities in optical trapping may produce heating of the optical components, thus causing optical drift, increased stabilization time, and/or decreased spatial resolution. As an example, reaching basepair resolution in optical tweezers experiments on DNA was facilitated by the use of milliKelvin temperature-stabilized objective [44]. Finally, judicious design and analysis of the experiment is required when large temperature fluctuations are anticipated. Among other issues, the reliability of (real-time) calibration of optical tweezers based on Brownian fluctuations is impacted by significant temperature changes.

3.3 Position and Force Detection

The key to quantitative optical trapping is accurate detection of the position of the particle in an optical trap. Within the volume of the laser focus, the displacement of the particle from its equilibrium position is directly proportional to the forces acting on this particle.

Lateral Position and Force Detection The simplest position-detection scheme relies on video-based imaging of a bead in the optical trap. Using centroid-tracking or template-matching algorithms, the position of one or multiple beads can be obtained with sub-pixel resolution (down to several nanometers) by digital video analysis [45, 46]. The most common position detection scheme is currently back-focal-plane interferometry, which typically provides the highest time resolution (~μs) and spatial resolution (~pm) [47, 48]. Here, the interference between unscattered and forward-scattered light of a laser beam focused on a bead is used to provide positional information in the two lateral dimensions. By imaging the intensity distribution in the back focal plane of a

condenser lens on a detector (such as a quadrant-photodiode (QPD) or position sensitive detector (PSD)), the recorded signals are insensitive to the location of the trap in the field of view. A major advantage of this technique is the use of the trapping laser to perform trapping and position detection simultaneously, hence the force detection and trap position are intrinsically aligned. In such arrangement, only relative displacements of the bead with respect to the trap are measured: displacements of up to a few hundred nanometers away from the center of the optical trap are directly proportional to the measured shift on the detectors in this configuration. On top of this, simultaneous video analysis of optical images can still be used to measure absolute positions and distances in the studied system.

Axial Position Detection True three-dimensional position detection allows tracking the (suppressed) Brownian motion of the trapped particle and thereby fully quantifying the forces felt by the object in the optical trap. This can be accomplished by combining axial position detection with the abovementioned lateral position detection techniques. The axial position of trapped particles can be detected by using fluorescence methods, performing template-based analysis of bead images (as in magnetic tweezers [49] or acoustic force spectroscopy [50] experiments, see Chapters 18 and 22), measuring the forward scattered light intensity, or by using non-imaging interference methods [6]. The non-imaging axial interference method, in which modulations in the total laser intensity are detected in the back focal plane of the condenser, is the most practical due to its accuracy and ease of integration with lateral interference-based detection. Contrary to lateral detection, the best axial sensitivity is obtained when only the low-NA fraction of the light is detected [51].

3.4 Trap Steering

In case the microscope stage movement range does not provide enough flexibility, the trapping beam itself can be steered through the sample. This is particularly useful for steering multiple optical traps. Lateral trap movement can be achieved by changing the incoming angle of the trapping beam into the objective, while the axial movement is affected by changing the level of collimation of the beam.

In practice, such three-dimensional trap steering can be accomplished by moving the lenses in a telescope in front of the objective. Alternatively, the use of tip-tilt or galvanometric mirrors, with accurate and reproducible positioning, allows rapid lateral trap movement up to several kHz. Finally, trap steering can also be accomplished using acousto-optical deflectors and electro-optical deflectors that provide higher scanning speeds up to the MHz range. It is important to realize that trapped objects are limited in manipulation speed as viscous drag will remove the trapped particle from the trap at high steering speeds.

A single laser source can be used to generate multiple traps by rapidly alternating the position of the laser between separate locations in a sample cell: if the laser is scanned rapidly enough, the trapped particles may not sense the transient absence of the optical trap. This way of generating multiple traps is called trap multiplexing or "time-sharing" [7, 52]. Time-shared optical traps provide large flexibility in the number of traps but typically require additional feedback electronics to compensate for deflection-dependent variations in trap stiffness. An alternative approach to generate multiple traps from a single laser line is provided by diffractive optical elements such as spatial light modulators (SLMs). Multiple trap generation and steering in this case relies on the holographic pattern that causes the incident laser to diffract into separate foci in the sample. Holographic schemes based on SLMs are constrained in straightforward use of interferometric position and force sensing schemes.

3.5 Environment of the Setup

To ensure stability and high spatial resolution, the environment of the optical tweezers setup needs to be well controlled. Common precautions include the use of passively damping optical tables and temperature stabilization of the room within 0.5–0.1 K. Also, convection of the air in the optical pathway can induce beam deviations through local density fluctuations. These effects can be minimized either by enclosing the optical path, by reducing the optical path length, and by reducing the number of foci along the optical path, since the beam is more sensitive to local density fluctuations in these focal points. For the most demanding applications, optical tweezers instruments have been placed in acoustically isolated rooms with air conditioning equipment that filters out dust particles in the air. Although the ultimate resolution of a single base pair of DNA was first demonstrated using an instrument in which the ambient air was replaced by helium (less susceptible to density fluctuations), such resolution was later matched using a setup placed in ambient air [38, 53].

4 Optical Tweezers Approaches for Single-Molecule Analysis

Optical tweezers have been successfully employed in a wide range of applications in the fields of biology and biophysics. The simplest optical tweezers layout utilizes a single optical trap to perform quantitative force and/or extension analysis on biomolecular systems that are tethered between the trapped object and a fixed substrate (i.e., a glass slide or a bead held by a micropipette [17], *see* Fig. 2a–c). Such single trap layouts can, for example, be used to monitor and quantify biomolecular activity or perform force spectroscopy on a biopolymer such as DNA [11, 22]. Here, we discuss

the possibilities to customize the experimental approach to the biological system by using different assay configurations, measurement modes, or by combining optical tweezers with fluorescence microscopy techniques.

4.1 Measurement Modes

Optical tweezers analyses typically provide access to measurement and/or control of two parameters: force and extension (*see* Fig. 6a). Depending on the type of information that one wants to retrieve, the experiments can be performed in different measurement modes where the relationship between the two parameters is examined. For DNA–ligand interactions, the most common measurement modes include force-extension analysis (Fig. 6b), measurements at constant DNA extension (distance clamp, Fig. 6c) or measurements at constant force (force clamp, Fig. 6d).

During a force-extension measurement, the force is typically monitored while the position of one of the beads is varied to quantify the mechanical response of the tethered system; the force-extension curve contains information on the mechanical

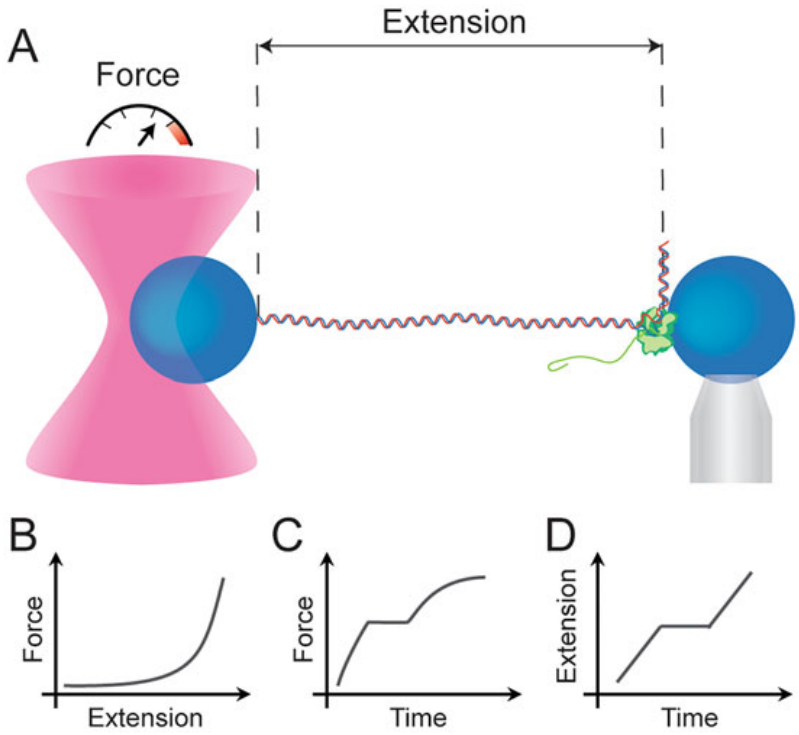

Fig. 6 Measurement modes in optical tweezers setups. (**a**) The two parameters that are experimentally accessible in a typical optical tweezers experiment are force and extension. (**b**–**d**) Representations of the data obtained through different measurement modes: (**b**) force-extension analysis (e.g., to quantify DNA mechanics [54]); (**c**) distance-clamp analysis (e.g., to analyze force-dependent filament assembly kinetics [58]); (**d**) force-clamp analysis (for example to monitor RNA polymerase activity [53]) (Reprinted with permission from Heller et al. [8]. Copyright 2014 American Chemical Society)

properties of the system. For nucleic acids, modelling the measured force-extension behavior using, for example, an extensible worm-like chain model (typically used for dsDNA) or a freely-jointed chain (suitable to model ssDNA), allows quantification of model parameters such as contour length and persistence length [54]. In turn, changes in these model parameters and/or in the mechanical response upon binding of nucleic acids by proteins can provide insight into the microscopic details of the nucleic-acid-protein interaction.

Measurements at constant DNA extension allow monitoring any changes in the force signal upon ligand binding and/or due to enzymatic activity, which can report on protein binding or activity in real time. The technical implementation of such a distance-clamp is rather straightforward. Caution is required, however, when using a distance-clamp to study force-dependent processes that are affected by the change in force over the course of the experiment (such as during a DNA polymerase activity assay [17, 28]).

A force-clamp experiment, on the other hand, utilizes active feedback to maintain a constant force by adjusting the tether extension in order to counter any changes in the measured force. Depending on the assay, substrate-stage movement, micropipette movement, or trap movement may be employed to maintain a constant force. In these experiments, the information-bearing signal is the change of tether extension over time. Force-clamping allows monitoring of ligand binding or enzymatic activity at a constant force in real time.

Variations to the measurement modes mentioned above may be used to optimize the experiment for the biological process or biophysical mechanism under scrutiny. An example of such an approach can be to do force-ramp measurements to perform a dynamic force spectroscopy analysis suitable to uncover details of, for example, the binding-energy landscape of DNA bridging ligands that may otherwise remain hidden [25]. Another example is the use of optical tweezers for microrheology assays, in which oscillatory movement of the trapped bead is used to assess the local visco-elastic properties in the direct vicinity of a trapped object or the visco-elastic response of the tethered object itself [55].

4.2 Biological Assays in Optical Tweezers

Over the last three decades, several optical trapping geometries have been explored, each adapted to the relevant biological system under investigation. Here, we discuss the most common assays, with illustrations omitting the trapping beam cones for simplicity (Fig. 7).

Translocation Assay Optical tweezers are very well suited to probe force generation or force-dependent translocation by molecular motors. In such an assay, the motor protein may be attached to an optically trapped bead, whereas the motor track (e.g., the DNA

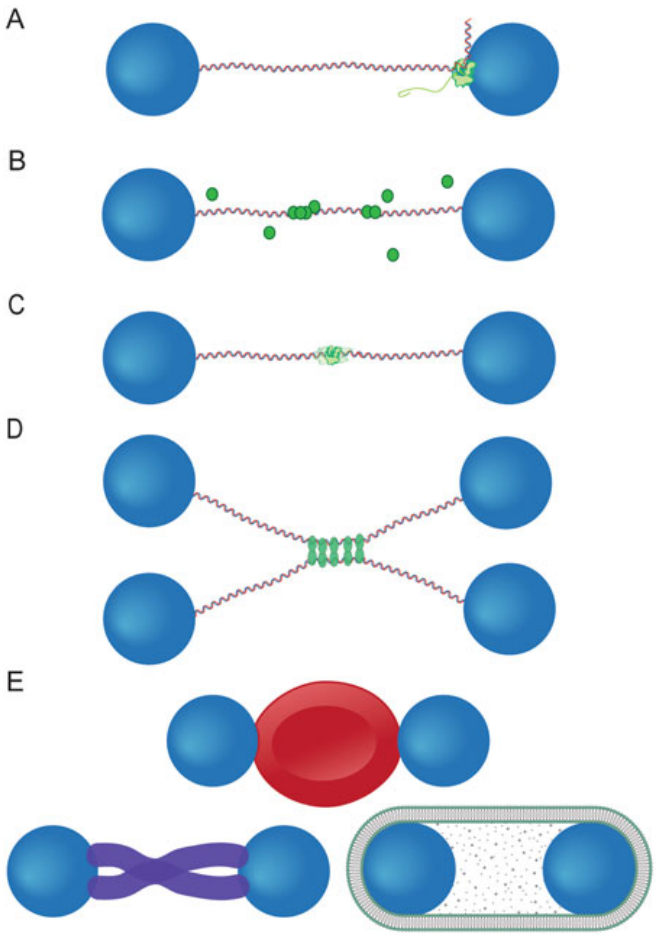

Fig. 7 Examples of biological assays that can be measured using optical tweezers—blue circles signify the optically trapped bead, whereas laser cones are omitted for clarity. (**a**) Translocation assay in a dual trap setup; (**b**) structural-change-based assay; (**c**) protein unfolding assay; (**d**) dual DNA assay; (**e**) examples of other optical tweezers assays, modified for experiments involving cells, chromosomes, or membranes (Adapted with permission from Heller et al. [8]. Copyright 2014 American Chemical Society)

or a microtubule) is either anchored to the surface or attached to the other trapped bead (Figs. 2a and 7a). In a force clamp measurement, the measured displacement can directly reflect the translocation of the motor protein under assisting or opposing load. Such translocation analyses have been used to quantify the stepping of kinesin [11, 15, 40] and RNA polymerases [22, 53] and hence inform on the thermodynamic and kinetic parameters of the mechanochemical cycle of the investigated motors.

Mechanical Change-Based Assay When DNA-binding proteins or other ligands impact mechanical properties of the tether, such as the contour length or persistence length, optical tweezers analyses can be used to quantify this mechanical impact (Fig. 7b). In this assay, the measured signal is the altered mechanical response of the

DNA molecule that can be caused, for example, by the interconversion between dsDNA and ssDNA (i.e., exonucleolysis), local structural changes (i.e., DNA bending), or coating the DNA with protein filaments that increase the rigidity of the polymer. This assay can be easily adapted to different biological problems involving DNA compaction [25, 56], dsDNA unwinding [14, 57], and many more [17, 58–61].

Unfolding Assay Optical tweezers are very well equipped to quantify force-induced structural alterations such as occur in a protein unfolding assay. Here, DNA can function as linker that extends the tether away from the surface of the bead (Fig. 7c). This assay has been successfully applied to study protein unfolding [62, 63] and opening of DNA/RNA structures (including DNA origami) [64–66] and has been employed for mechanical fingerprinting with nano-calipers [67].

Dual DNA Assay For geometrically or architecturally more complex analyses, it is possible to manipulate two DNA molecules independently (Fig. 7d). Such an assay provides additional geometrical control that can be used to study (protein-mediated) DNA–DNA interactions or more complex two- or three-dimensional molecular architectures that go beyond that of a single one-dimensional tether. This level of control can be obtained through lateral position control of four optical traps. Furthermore, the ability to reposition at least one of the traps in the axial direction allows, for example, controlled braiding or entanglement of two DNA strands. This type of assay has been successful in mimicking the in vivo contacts between DNA, aiding research of molecular mechanism of DNA bridging proteins [25, 30], topological changes in presence of topoisomerases [68], and quantitative analysis of protein repositioning due to intersegmental transfer [31, 32].

Optically trapped beads can furthermore be used to probe the viscoelastic force response of considerably larger objects, such as cells [69, 70] or chromosomes [71] (*see* Fig. 7e and Chapter 5). Additionally, coating the beads with lipid membranes has been applied to study vesicle assemblies [72] and membrane bridging complexes [73]. Finally, a range of other applications that go beyond single-molecule analyses have been enabled by optical tweezers. For example, optical tweezers have been demonstrated in studies of biomolecular systems in vivo, and time-shared optical trapping has been employed to manipulate large biological structures and to manipulate larger assemblies of colloidal particles (you can find some fun examples on YouTube) [74–77].

4.3 Combining Optical Tweezers with Fluorescence Microscopy

Fluorescence microscopy is a powerful method that has continuously enhanced our understanding of biological systems (see Chapter 6) by retrieving spatially and/or temporally resolved information of labeled (bio)molecules. Since fluorescence microscopy typically provides a different type of information than optical tweezers do, combining these two methods can have clear complementary or synergistic advantages, enabling investigations that cannot be performed with the individual methods [8, 35, 78–80]. The direct visualization of single molecules in controlled optical tweezers manipulation experiments has indeed proven to be a powerful method for the detailed investigation of biomolecular systems, in particular for unraveling DNA–protein interactions [35, 58, 81]. In these experiments, DNA is manipulated with optical tweezers, while local and specific information on the binding and activity of proteins interacting with the DNA can be obtained concurrently through fluorescence microscopy. Changes in DNA structure due to DNA-protein interactions or movement of proteins along DNA can thus be simultaneously studied with force spectroscopy and fluorescence microscopy, providing a high level of versatility, unambiguity, and synergy in these experiments [82].

One of the first instruments that combined optical tweezers with fluorescence imaging was based on the total-internal reflection fluorescence (TIRF) microscopy, as pictured on Fig. 8a [83]. Since, in TIRF microscopy, the evanescent wave only excites molecules that reside within ~100 nm of the glass substrate, this technique limits unwanted background fluorescence, hence allowing single-molecule analyses to be performed at higher background concentrations of fluorescent molecules than is possible with other imaging techniques [83, 84]. However, as the trapped microbeads are usually considerably larger in size than the ~100 nm illumination depth, the geometry of this setup restricts the freedom to manipulate the system and move around in the sample cell.

Conventional wide-field fluorescence microscopy (*see* Fig. 8b), on the other hand, provides robust and straightforward imaging capabilities in optical tweezers by employing camera-based fluorescence imaging and a wide fluorescence excitation beam that illuminates a large field of view. At elevated concentrations of fluorescently labeled proteins, however, wide-field fluorescence can suffer from out-of-focus fluorescence excitation and detection, which restricts the conditions under which single-molecule fluorescence can be resolved. Nonetheless, the approach has proven to be very successful in studying a wide range of biomolecular systems [58, 60, 85].

Confocal fluorescence microscopy does provide background rejection by focusing the excitation beam into a diffraction limited spot and employing fluorescence detection through a confocal pinhole (Fig. 8c). This technique allows for imaging at relatively high fluorophore concentrations (20–100 nM), but it requires line or raster scanning the confocal spot to obtain a one- or

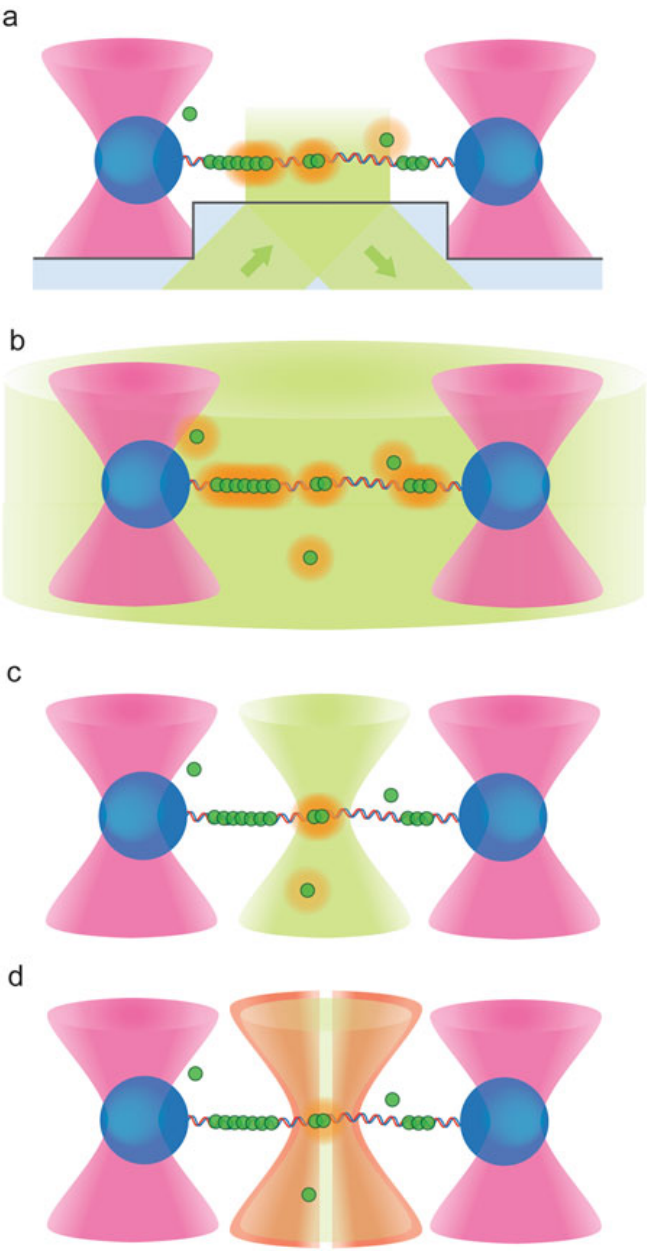

Fig. 8 Fluorescence microscopy techniques combined with optical tweezers: (**a**) total internal-reflection fluorescence microscopy (TIRF); (**b**) wide-field fluorescence microscopy; (**c**) confocal fluorescence microscopy; (**d**) stimulated emission depletion (STED) microscopy (Adapted with permission from Heller et al. [8]. Copyright 2014 American Chemical Society)

two-dimensional image of the optically stretched construct. Due to prior knowledge of the location of the DNA (e.g., in between two optical traps), rapid one-dimensional scanning typically suffices to monitor biomolecular activity along the DNA, thus alleviating the necessity to perform slower two-dimensional raster scans. Furthermore, point-confocal measurements at a site of interest along the tether can inform on local binding/unbinding or changes in FRET signal with high temporal resolution (sub-millisecond) [86, 87].

All of the three aforementioned fluorescence imaging methods are limited to a spatial resolution of 200–300 nm (depending on the wavelength) due to the diffraction-limit. The advent of super-resolution microscopy techniques, however, circumvents this limit. Optical tweezers combined with stimulated emission depletion microscopy (STED, *see* Fig. 8d) provide the ability to directly observe and study the kinetics of DNA binders with a resolution of 50 nm [88]. Alternatively, localization-based super-resolution methods such as photoactivated localization microscopy (PALM) have also been successfully combined with optical tweezers analysis [89], and the use of DNA intercalators in inverse binding-activated localization microscopy (iBALM) was shown to enable imaging of non-fluorescent DNA binders with super-resolution [89, 90]. The elevated molecular densities that become accessible through super-resolution microscopy allow linking idealized in vitro conditions with the dense and crowded situation in vivo [88].

Other advanced optical microscopy techniques such as fluorescence polarization imaging and Förster resonance energy transfer (FRET) have also been successfully combined with optical tweezers [59, 78, 86, 91, 92]. New possibilities of these combinations include study of, for example, the spatial and temporal dynamics of DNA repair processes [30, 32, 58] and structure-function relationships of DNA-binding enzymes [78].

5 Commercial Optical Tweezers Systems

The design and construction of an optical tweezers instrument can be a challenging task, requiring practical experience and theoretical knowledge in fields ranging from laser physics to computer science. During the past decade, several companies have started offering commercial solutions for optical trapping experiments, which now enables a wide range of researchers to exploit the benefits of optical tweezers analyses. These solutions range from do-it-yourself kits to fully automated turn-key platforms, including instruments that can be flexibly attached or integrated into a standard inverted optical microscope, as well as stand-alone systems that are optimized for optical tweezers operation or concurrent optical trapping and fluorescence microscopy. Furthermore, broader adoption of optical tweezers in biomolecular research fields goes hand in hand with the increasing availability of (open source, commercial, and/or standardized) data analysis software, which is critical for exploitation of any optical tweezers experiment.

When considering the purchase of a commercial optical tweezers instrument, several aspects should be kept in mind. Obviously, the first thing to define is the main biological application or application range of the instrument, whether that concerns

micromanipulation, high-resolution force spectroscopy, hardware and/or software integration, or fluorescence imaging. Finally, throughput and workflow can also become particularly important features in single-molecule analyses that face the task of gathering large statistics on a molecule-by-molecule basis.

6 Concluding Remarks

Optical tweezers techniques form an invaluable addition to the single-molecule toolkit. These minimally invasive techniques provide scientists with the ability to actively manipulate biomolecules with (sub)nanometer precision, and to measure or apply forces with (sub)picoNewton resolution. Examples of the application of these powerful tools in molecular biology include the studies of active molecular motors, the mechanical properties of DNA, and the mechanochemistry of DNA–protein interactions. Commercial optical tweezers systems are becoming increasingly available, which makes this powerful and versatile technique accessible to a broad range of researchers from different backgrounds and will undoubtedly drive new biological discoveries on the single-molecule level. The following chapters will describe detailed methods and protocols of several applications of optical tweezers in molecular biology.

7 Notes

1. It is important to note that, in practice, the detector used to determine the bead position reads *uncalibrated* displacement fluctuations $u(t)$ (i.e., as some voltage rather than as a displacement in nanometers). The response of the detector R, which has units m/V, relates the displacement to $u(t)$ as $x(t) = Ru(t)$. To fully calibrate an optical trap, the power spectrum of the uncalibrated displacement fluctuations $S_u(f)$ is fitted with a Lorentzian:

$$S_u(f) = \frac{S_{u,0} {f_c}^2}{\left({f_c}^2 + f^2\right)},$$

Once the parameters $S_{u,\,0}$and f_c are obtained, the trap stiffness can be calculated using

$$\kappa = \frac{2k_BT}{\pi S_{u,0} f_c} \text{ or } \kappa = 2\pi\gamma f_c,$$

and, providing the bead diameter and solvent viscosity are known, the detector response can be calculated using

$$R = \left[\frac{k_B T}{\pi^2 \gamma S_{u,0} {f_c}^2}\right]^{\frac{1}{2}} \underset{25\,^\circ\mathrm{C}}{\Rightarrow} \left[\frac{5.0 \times 10^{-20}\ m^3 s^{-1}}{S_{u,0} {f_c}^2 d}\right]^{\frac{1}{2}}.$$

Finally, to convert uncalibrated displacement data to forces, the displacement signal should be multiplied by R and the trap stiffness, such that, $F = -\kappa x = -\kappa R u$.

Competing Interest Statement

IH, EJGP, and GJLW declare a financial interest in LUMICKS B.V. AMM and JM declare no competing financial interest.

References

1. Ashkin A (1970) Acceleration and trapping of particles by radiation pressure. Phys Rev Lett 24:156–159
2. Ashkin A, Dziedzic JM, Bjorkholm JE et al (1986) Observation of a single-beam gradient force optical trap for dielectric particles. Opt Lett 11:288
3. Chu S (1991) Laser manipulation of atoms and particles. Science 253:861–866
4. Chu S (1992) Laser trapping of neutral particles. Sci Am 266:70–76
5. Svoboda K, Block SM (1994) Biological applications of optical forces. Annu Rev Biophys Biomol Struct 23:247–285
6. Neuman KC, Block SM (2004) Optical trapping. Rev Sci Instrum 75:2787
7. Moffitt JR, Chemla YR, Smith SB et al (2008) Recent advances in optical tweezers. Annu Rev Biochem 77:205–228
8. Heller I, Hoekstra TP, King GA et al (2014) Optical tweezers analysis of DNA-protein complexes. Chem Rev 114:3087–3119
9. Ashkin A, Dziedzic J (1987) Optical trapping and manipulation of viruses and bacteria. Science 235:1517–1520
10. Ashkin A, Dziedzic JM, Yamane T (1987) Optical trapping and manipulation of single cells using infrared laser beams. Nature 330: 769–771
11. Block SM, Goldstein LSB, Schnapp BJ (1990) Bead movement by single kinesin molecules studied with optical tweezers. Nature 348: 348–352
12. Bustamante C, Macosko JC, Wuite GJL (2000) Grabbing the cat by the tail: manipulating molecules one by one. Nat Rev Mol Cell Biol 1:130–136
13. Davenport RJ, Wuite GJ, Landick R et al (2000) Single-molecule study of transcriptional pausing and arrest by E. coli RNA polymerase. Science 287:2497–2500
14. Smith SB, Cui Y, Bustamante C (1996) Overstretching B-DNA: the elastic response of individual double-stranded and single-stranded DNA molecules. Science 271:795–799
15. Svoboda K, Schmidt CF, Schnapp BJ et al (1993) Direct observation of kinesin stepping by optical trapping interferometry. Nature 365:721–727
16. Zamft B, Bintu L, Ishibashi T et al (2012) Nascent RNA structure modulates the transcriptional dynamics of RNA polymerases. Proc Natl Acad Sci U S A 109:8948–8953
17. Wuite GJL, Smith SB, Young M et al (2000) Single-molecule studies of the effect of template tension on T7 DNA polymerase activity. Nature 404:103–106
18. Essevaz-Roulet B, Bockelmann U, Heslot F (1997) Mechanical separation of the complementary strands of DNA. Proc Natl Acad Sci 94:11935–11940
19. Kellermayer MS (1997) Folding-unfolding transitions in single titin molecules characterized with laser tweezers. Science 276:1112–1116
20. Tskhovrebova L, Trinick J, Sleep JA et al (1997) Elasticity and unfolding of single molecules of the giant muscle protein titin. Nature 387:308–312
21. Wang MD, Schnitzer MJ, Yin H et al (1998) Force and velocity measured for single

molecules of RNA polymerase. Science 282: 902–907
22. Yin H, Wang MD, Svoboda K et al (1995) Transcription against an applied force. Science 270:1653–1657
23. Bustamante C, Bryant Z, Smith SB (2003) Ten years of tension: single-molecule DNA mechanics. Nature 421:423–427
24. Gross P, Laurens N, Oddershede LB et al (2011) Quantifying how DNA stretches, melts and changes twist under tension. Nat Phys 7:731–736
25. Dame RT, Noom MC, Wuite GJL (2006) Bacterial chromatin organization by H-NS protein unravelled using dual DNA manipulation. Nature 444:387–390
26. Neupane K, Foster DAN, Dee DR et al (2016) Direct observation of transition paths during the folding of proteins and nucleic acids. Science 352:239–242
27. Woodside MT, Block SM (2014) Reconstructing folding energy landscapes by single-molecule force spectroscopy. Annu Rev Biophys 43:19–39
28. Hoekstra TP, Depken M, Lin S-N et al (2017) Switching between exonucleolysis and replication by T7 DNA polymerase ensures high Fidelity. Biophys J 112:575–583
29. Laurens N, Driessen RPC, Heller I et al (2012) Alba shapes the archaeal genome using a delicate balance of bridging and stiffening the DNA. Nat Commun 3:1328
30. Brouwer I, Sitters G, Candelli A et al (2016) Sliding sleeves of XRCC4–XLF bridge DNA and connect fragments of broken DNA. Nature 535:566–569
31. Van Den Broek B, Lomholt MA, Kalisch SMJ et al (2008) How DNA coiling enhances target localization by proteins. Proc Natl Acad Sci U S A 105:15738–15742
32. Forget AL, Kowalczykowski SC (2012) Single-molecule imaging of DNA pairing by RecA reveals a three-dimensional homology search. Nature 482:423–427
33. Gross P, Farge G, Peterman EJG et al (2010) Combining optical tweezers, single-molecule fluorescence microscopy, and microfluidics for studies of DNA-protein interactions. Methods Enzymol 475:427–453
34. Brewer LR, Bianco PR (2008) Laminar flow cells for single-molecule studies of DNA-protein interactions. Nat Methods 5: 517–525
35. van Mameren J, Peterman EJG, Wuite GJL (2008) See me, feel me: methods to concurrently visualize and manipulate single DNA molecules and associated proteins. Nucleic Acids Res 36:4381–4389
36. Ashkin A (1992) Forces of a single-beam gradient laser trap on a dielectric sphere in the ray optics regime. Biophys J 61:569–582
37. Gittes F, Schmidt CF (1998) Signals and noise in micromechanical measurements. Methods Cell Biol 55:129–156
38. Moffitt JR, Chemla YR, Izhaky D et al (2006) Differential detection of dual traps improves the spatial resolution of optical tweezers. Proc Natl Acad Sci U S A 103:9006–9011
39. Peterman EJG, Gittes F, Schmidt CF (2003) Laser-induced heating in optical traps. Biophys J 84:1308–1316
40. Sudhakar S, Abdosamadi MK, Jachowski TJ et al (2021) Germanium nanospheres for ultraresolution picotensiometry of kinesin motors. Science 371:eabd9944
41. Vermeulen KC, Wuite GJL, Stienen GJM et al (2006) Optical trap stiffness in the presence and absence of spherical aberrations. Appl Opt 45:1812
42. Reihani SNS, Mir SA, Richardson AC et al (2011) Significant improvement of optical traps by tuning standard water immersion objectives. J Opt 13:105301
43. Guck J, Ananthakrishnan R, Mahmood H et al (2001) The optical stretcher: a novel laser tool to micromanipulate cells. Biophys J 81:767–784
44. Mahamdeh M, Schäffer E (2009) Optical tweezers with millikelvin precision of temperature-controlled objectives and base-pair resolution. Opt Express 17:17190
45. Cheezum MK, Walker WF, Guilford WH (2001) Quantitative comparison of algorithms for tracking single fluorescent particles. Biophys J 81:2378–2388
46. Crocker JC, Grier DG (1996) Methods of digital video microscopy for colloidal studies. J Colloid Interface Sci 179:298–310
47. Denk W, Webb WW (1990) Optical measurement of picometer displacements of transparent microscopic objects. Appl Opt 29:2382
48. Gittes F, Schmidt CF (1998) Interference model for back-focal-plane displacement detection in optical tweezers. Opt Lett 23:7–9
49. De Vlaminck I, Dekker C (2012) Recent advances in magnetic tweezers. Annu Rev Biophys 41:453–472
50. Sitters G, Kamsma D, Thalhammer G et al (2014) Acoustic force spectroscopy. Nat Methods 12:47–50
51. Dreyer JK, Berg-Sørensen K, Oddershede L (2004) Improved axial position detection in

optical tweezers measurements. Appl Opt 43: 1991

52. Capitanio M, Cicchi R, Saverio Pavone F (2007) Continuous and time-shared multiple optical tweezers for the study of single motor proteins. Opt Lasers Eng 45:450–457
53. Abbondanzieri EA, Greenleaf WJ, Shaevitz JW et al (2005) Direct observation of base-pair stepping by RNA polymerase. Nature 438: 460–465
54. Bustamante C, Bryant Z, Smith SB (2003) Ten years of tension: single-molecule DNA mechanics DNA as a worm-like chain. Feature Nat 421:423–427
55. Turlier H, Fedosov DA, Audoly B et al (2016) Equilibrium physics breakdown reveals the active nature of red blood cell flickering. Nat Phys 12:513–519
56. Cui Y, Bustamante C (2000) Pulling a single chromatin fiber reveals the forces that maintain its higher-order structure. Proc Natl Acad Sci U S A 97:127–132
57. King GA, Peterman EJG, Wuite GJL (2016) Unravelling the structural plasticity of stretched DNA under torsional constraint. Nat Commun 7:11810
58. van Mameren J, Modesti M, Kanaar R et al (2009) Counting RAD51 proteins disassembling from nucleoprotein filaments under tension. Nature 457:745–748
59. Backer AS, Biebricher AS, King GA et al (2019) Single-molecule polarization microscopy of DNA intercalators sheds light on the structure of S-DNA. Sci Adv 5:eaav1083
60. Biebricher A, Wende W, Escudé C et al (2009) Tracking of single quantum dot labeled EcoRV sliding along DNA manipulated by double optical tweezers. Biophys J 96:L50–L52
61. Biebricher AS, Heller I, Roijmans RFH et al (2015) The impact of DNA intercalators on DNA and DNA-processing enzymes elucidated through force-dependent binding kinetics. Nat Commun 6:7304
62. Cecconi C, Shank EA, Bustamante C et al (2005) Direct observation of the three-state folding of a single protein molecule. Science 309:2057–2060
63. Rico-Pasto M, Zaltron A, Davis SJ et al (2022) Molten globule–like transition state of protein barnase measured with calorimetric force spectroscopy. Proc Natl Acad Sci 119: e2112382119
64. Liphardt J, Onoa B, Smith SB et al (2001) Reversible unfolding of single RNA molecules by mechanical force. Science 292:733–737
65. Dumont S, Cheng W, Serebrov V et al (2006) RNA translocation and unwinding mechanism of HCV NS3 helicase and its coordination by ATP. Nature 439:105–108
66. Karna D, Pan W, Pandey S et al (2021) Mechanochemical properties of DNA origami nanosprings revealed by force jumps in optical tweezers. Nanoscale 13:8425–8430
67. Shrestha P, Yang D, Tomov TE et al (2021) Single-molecule mechanical fingerprinting with DNA nanoswitch calipers. Nat Nanotechnol 16:1362–1370
68. Bakx JAM, Biebricher AS, King GA et al (2022) Duplex DNA and BLM regulate gate opening by the human TopoIIIα-RMI1-RMI2 complex. Nat Commun 13:584
69. Li J, Dao M, Lim CT et al (2005) Spectrin-level modeling of the cytoskeleton and optical tweezers stretching of the erythrocyte. Biophys J 88:3707–3719
70. Hendricks AG, Holzbaur ELF, Goldman YE (2012) Force measurements on cargoes in living cells reveal collective dynamics of microtubule motors. Proc Natl Acad Sci 109:18447–18452
71. Meijering AEC, Sarlós K, Nielsen CF et al (2022) Nonlinear mechanics of human mitotic chromosomes. Nature 605:545–550
72. Bolognesi G, Friddin MS, Salehi-Reyhani A et al (2018) Sculpting and fusing biomimetic vesicle networks using optical tweezers. Nat Commun 9:1882
73. Brouwer I, Giniatullina A, Laurens N et al (2015) Direct quantitative detection of Doc2b-induced hemifusion in optically trapped membranes. Nat Commun 6:8387
74. Grier DG (2003) A revolution in optical manipulation. Nature 424:810–816
75. Liesener J, Reicherter M, Haist T et al (2000) Multi-functional optical tweezers using computer-generated holograms. Opt Commun 185:77–82
76. Mio C, Gong T, Terray A et al (2000) Design of a scanning laser optical trap for multiparticle manipulation. Rev Sci Instrum 71:2196
77. Visscher K, Brakenhoff GJ, Krol JJ (1993) Micromanipulation by "multiple" optical traps created by a single fast scanning trap integrated with the bilateral confocal scanning laser microscope. Cytometry 14:105–114
78. Comstock MJ, Whitley KD, Jia H et al (2015) Direct observation of structure-function relationship in a nucleic acid-processing enzyme. Science 348:352–354

79. Comstock MJ, Ha T, Chemla YR (2011) Ultrahigh-resolution optical trap with single-fluorophore sensitivity. Nat Methods 8:335–340
80. Heller I, Sitters G, Broekmans OD et al (2014) Mobility analysis of super-resolved proteins on optically stretched DNA: comparing imaging techniques and parameters. ChemPhysChem 15:727–733
81. van Mameren J, Gross P, Farge G et al (2009) Unraveling the structure of DNA during overstretching by using multicolor, single-molecule fluorescence imaging. Proc Natl Acad Sci 106: 18231–18236
82. King GA, Gross P, Bockelmann U et al (2013) Revealing the competition between peeled ssDNA, melting bubbles, and S-DNA during DNA overstretching using fluorescence microscopy. Proc Natl Acad Sci U S A 110: 3859–3864
83. Harada Y, Funatsu T, Murakami K et al (1999) Single-molecule imaging of RNA polymerase-DNA interactions in real time. Biophys J 76: 709–715
84. Lang MJ, Fordyce PM, Engh AM et al (2004) Simultaneous, coincident optical trapping and single-molecule fluorescence. Nat Methods 1: 133–139
85. Candelli A, Wuite GJL, Peterman EJG (2011) Combining optical trapping, fluorescence microscopy and micro-fluidics for single molecule studies of DNA-protein interactions. Phys Chem Chem Phys 13:7263–7272
86. Hohng S, Zhou R, Nahas MK et al (2007) Fluorescence-force spectroscopy maps two-dimensional reaction landscape of the Holliday junction. Science 318:279–283
87. Sirinakis G, Ren Y, Gao Y et al (2012) Combined versatile high-resolution optical tweezers and single-molecule fluorescence microscopy. Rev Sci Instrum 83:093708
88. Heller I, Sitters G, Broekmans OD et al (2013) STED nanoscopy combined with optical tweezers reveals protein dynamics on densely covered DNA. Nat Methods 10:910–916
89. Patterson G, Davidson M, Manley S et al (2010) Superresolution imaging using single-molecule localization. Annu Rev Phys Chem 61:345–367
90. Meijering AEC, Biebricher AS, Sitters G et al (2020) Imaging unlabeled proteins on DNA with super-resolution. Nucleic Acids Res 48: e34–e34
91. Murade CU, Subramaniam V, Otto C et al (2010) Force spectroscopy and fluorescence microscopy of dsDNA-YOYO-1 complexes: implications for the structure of dsDNA in the overstretching region. Nucleic Acids Res 38:3423–3431
92. Bennink ML, Scharer OD, Kanaar R et al (1999) Single-molecule manipulation of double-stranded DNA using optical tweezers: interaction studies of DNA with RecA and YOYO-1. Cytometry 36:200–208